PCCP

ROYAL SOCIETY OF CHEMISTRY

PAPER

View Article Online
View Journal | View Issue

Cite this: *Phys. Chem. Chem. Phys.*, 2025, **27**, 14555

Component-wise AO basis reduction: norm loss, negative contribution normalization, and functional implications†

Mindaugas Macernis *

Atomic orbital (AO) normalization is a foundational assumption in electronic structure theory, yet in practice, the norm of contracted basis functions can deviate from unity due to internal reduction and transformation mechanisms applied by quantum chemistry packages. This work presents a systematic framework for analyzing the physical and numerical consequences of primitive basis function elimination and AO-level norm inconsistency. The implemented methodology quantifies norm loss, separates constructive and destructive contributions, and enables precise renormalization by retaining both positive and negative terms within AO representations. Using two representative systems—a Raman-active carotenoid (lycopene) and a phosphorus dimer with through-space *J*(P–P) coupling—sensitivity to AO normalization was evaluated. While vibrational frequencies remained stable across normalization schemes, Raman intensities and *J*-coupling constants showed non-negligible shifts: up to 6 Hz for phosphorus and over 50 units in Raman activity. The results demonstrate that AO normalization is not merely a numerical refinement, but a physically impactful step with implications for precision spectroscopy and quantum computing applications.

Received 4th May 2025,
Accepted 16th June 2025

DOI: 10.1039/d5cp01681a

rsc.li/pccp

Introduction

The accuracy of quantum chemical methods depends mainly on three general features such as the choice of the Hamiltonian, approximate treatment of electron correlation by truncating the many-particle Hilbert space, and the definition of the basis set determining the one-particle orbital representation.[1,2] Regardless of the level of theory, an insufficient basis set yields erroneous results, whereas an appropriate basis set can be expected to produce at least qualitatively correct results.

Gaussian-type orbitals (GTOs), centered on atomic nuclei, are commonly used as basis functions in the linear combination of atomic orbitals (LCAO) method.[1,3,4] Generally contracted basis sets include the correlation-consistent (cc) families proposed by Dunning & coworkers,[5–12] widely used in the form of cc-pVXZ (X = D, T, Q, 5, 6), where X denotes the number of contracted Gaussian-type orbitals (CGTOs) used to represent each occupied atomic orbital. These sets can be systematically extended with diffuse functions, denoted by aug-, d-aug-, and t-aug-prefixes for singly, doubly, and triply augmented variants.

Another general contraction approach is the atomic natural orbital (ANO) basis set, in which the contraction coefficients are obtained by optimizing atomic energies.[13] Optimized atomic Slater-type orbitals (STOs) were often approximated by fixed linear combinations of Gaussian functions,[14] forming the basis of widely used Pople-type basis sets such as 3-21G and 6-311G.[15–17] Basically, molecular orbitals have a functional[2,18] form given by equation:

$$\varphi = Y_{lm} \sum_i C_i \sum_j C_{ij} e^{-\varsigma_{ij} r^2} \quad (1)$$

Where the correct symmetry (s, p, *etc.*) orbital gives the Y_{lm} function and the Gaussian primitive function is e^{-r^2}. The contraction coefficients C_{ij} and exponents ς_{ij} are read from a database and should not change over the calculation.[2] Thus, basis sets are typically provided as contracted functions in segmented form, meaning that quantum chemistry packages are responsible for normalizing each atomic orbital.

The effects of basis set reduction have been extensively studied across multiple quantum chemical methods---including density functional theory (DFT), Hartree–Fock (HF), and coupled-cluster (CC)-to improve accuracy or reduce computational cost.[18–34] However, studies targeting high-precision results[26,30,31,35–46] or analysing basis set superposition errors (BSSE)[35–37,40,43,46] often face reproducibility challenges due to undocumented and automatically applied normalization procedures, as demonstrated in this work. Notably, the widely used cc-pVDZ basis set provides a clear example of predefined reductions embedded in default system libraries, despite its

Institute of Chemical Physics, Vilnius University, Saulėtekio av. 3, Vilnius, LT-10257, Lithuania. E-mail: mindaugas.macernis@ff.vu.lt

† Electronic supplementary information (ESI) available. See DOI: https://doi.org/10.1039/d5cp01681a

frequent use in high-accuracy applications.[30,39–42,44–46] For this reason, cc-pVDZ was selected as a test case to evaluate how AO reduction and normalization affect computed results.

This paper introduces a framework for evaluating the physical and numerical effects of primitive Gaussian basis function elimination. Norm loss and component-level analysis reveal that atomic orbital (AO) pruning—often applied automatically and without user control—can impact computed molecular properties. AO normalization is revisited through the separation of positive and negative contraction contributions, representing constructive and destructive superposition components.

A case study using the cc-pVDZ[5,47] basis set is presented for hydrogen, carbon, and phosphorus, elements selected for their typical angular momentum behaviour and susceptibility to internal reduction in system libraries. Calculations were performed using Gaussian,[48] which enables explicit basis input and reflects normalization behaviour during SCF processing. The study assesses the impact of normalization strategies on total energies, dipole moments, Raman intensities, and J(P–P) couplings.

Two representative systems were selected to assess the physical implications of AO normalization: lycopene (LYC), a conjugated carotenoid (Car) with well-defined Raman-active modes,[49–53] and bis(diphenylphosphino)methane (dppm), which enables through-space P–P spin–spin coupling relevant to quantum computing[54–58] and other studies.[59] These molecules provide sensitivity benchmarks for vibrational intensities and sub-Hz nuclear coupling constants.

All results are based on a reproducible methodology implemented in the open-source tool BasisSculpt, which supports precise and controlled AO normalization.

Results and discussion

Normalization theory and reduction of basis sets

The basis set representing contracted atomic orbitals must be normalized and can written as

$$\int_0^\infty [\phi(r)]^2 \cdot 4\pi r^2 \mathrm{d}r = 1 \tag{2}$$

The reduction procedure involves eliminating a single atomic orbital component, which ideally should only affect the total norm at the level of numerical noise or computational precision. For illustration, it can be considered reducing a three-term expansion to two terms:

$$\phi_{\text{full}} = c_1 N_1 \mathrm{e}^{-\alpha_1 r^2} + c_2 N_2 \mathrm{e}^{-\alpha_2 r^2} + c_3 N_3 \mathrm{e}^{-\alpha_3 r^2} \tag{3}$$

$$\phi_{\text{reduced}} = c_1 N_1 \mathrm{e}^{-\alpha_1 r^2} + c_2 N_2 \mathrm{e}^{-\alpha_2 r^2} \tag{4}$$

Renormalization should result in the integrals being almost equal:

$$\int |\phi_{\text{full}}|^2 \approx \int \left|\phi_{\text{reduced, normalized}}\right|^2 \tag{5}$$

However, the effect of the reduction is lost in this case, as both integrals are normalized to one. Therefore, the most informative approach is to compare the original and reduced integrals before renormalization. This allows for quantifying the relative contribution of the removed term as a percentage.

$$\delta_{\text{loss}} = \frac{\|\phi_{\text{full}}\|^2 - \|\phi_{\text{reduced}}\|^2}{\|\phi_{\text{full}}\|^2} \times 100\% \tag{6}$$

This raises the question of whether eliminating negative contraction coefficients is justified, given their suppressive contributions. In the normalization procedure, their impact is expected to be negligible if the coefficients are very small, and the total energy should remain unaffected. In such cases, renormalization may not be physically meaningful. However, when multiple negative contraction coefficients are involved, the function can be separated into constructive and destructive components.

$$\phi(r) = \phi_+(r) + \phi_-(r) \tag{7}$$

If renormalization is applied to only one component, the imbalance causes the remaining component to dominate, degrading the function's physical accuracy. Thus, normalization must be applied proportionally to all components to preserve the functional balance.

$$s_+^2 \cdot \|\phi_+\|^2 + s_-^2 \cdot \|\phi_-\|^2 + 2 s_+ s_- \cdot \langle \phi_+, \phi_- \rangle = 1 \tag{8}$$

A computational simplification involves splitting the normalization into two steps and verifying consistency between pre- and post-normalization values.

$$\text{Norm}_+ = \int \phi_+^2(r)\mathrm{d}r \tag{9}$$

$$\text{Norm}_- = \int \phi_-^2(r)\mathrm{d}r \tag{10}$$

However, it must be noted that

$$\|\phi\|^2 \neq \|\phi_+\|^2 + \|\phi_-\|^2 \tag{11}$$

and without including the cross-term

$$\langle \phi_+, \phi_- \rangle \tag{12}$$

separate normalization of positive and negative contribution leads to a function with incorrect total norma and unphysical shape. The requirement of projection-based normalization will restore phase interference and ensures both correct amplitude and function form.

From this point, a proportional analysis was performed to assess whether the atomic orbitals (AOs) in the basis set are appropriately normalized. This involves evaluating the total contribution of all Gaussian primitives constructing a given AO, regardless of whether the AO is defined across multiple blocks (*e.g.*, multiple entries for S orbitals).

Impact of primitive elimination and normalization on DFT results

In order to understand the effects of basis set reduction, the loss of norm resulting from both primitive-level and block-level eliminations should be qualified. The contribution of

individual Gaussian primitives was evaluated for each atomic orbital (AO) block, and their removal simulated.

However, when there are repeated α values across blocks the entire block can be reduced. In order to take this into account, the intra-block reduction effects on all selected AO blocks were treated as one joined block (Join-block). This technique allows calculation of the contribution of individual primitive Gaussian functions to the AO, based on their grouping into a Join-block.

Norm reduction was expressed as a percentage relative to the originally selected full block. The current analysis focuses on hydrogen (H), carbon (C), and phosphorus (P) atoms, which were chosen to investigate the effects of basis set normalization on molecular properties in the selected systems. The analysis was performed with cc-pVDZ taken from the basis set exchange.[60]

We used different cc-pVDZ basis set normalization approaches A1, A2, A3Exc and A4BS:

A1 – the typical basis set normalization as implemented in Gaussian software;[48]

A2 – the basis set normalization as implemented in Gaussian software by using the keyword which prevents basis set reduction;[48]

A3Exc – the typical basis set normalization as implemented in software[48] but with the basis set provided from the basis set exchange (BSE);[60]

A4BS – renormalized basis set by saving AO positive and negative contributions with BasisSculpt implementation by taking the basis set provided from the basis set exchange.[60]

The analysed normalization approaches – A1, A2, A3Exc, and A4BS – apply different reduction strategies. A3Exc uses the original cc-pVDZ basis set without any reduction. A4BS retains both constructive and destructive components after explicit normalization. In contrast, A2 provided by default within the internal system library, includes only initial reductions without renormalization. A1 applies[48] a more aggressive reduction strategy by using an A2-type basis set.

It should be noted that the initial basis set for A1 and A2 is the basis set from the internal Gaussian software database which has reduction applied already, for example: hydrogen has 3 α in the first block (AO labelled as S) while in A3Exc from BSE it has 4; carbon has 8 α in the first two blocks (AO labelled as S) while in BSE it is reported as 9, the forth block (AO labelled as P) has 3 α while in BSE there are 4; phosphorus has 11 α in the first three blocks (AO labelled as S) while in BSE it is reported as 12, the fifth and sixth blocks (AO labelled as P) have 7 α while in BSE there are 8.

Hydrogen. For the A1-type basis set normalization, hydrogen exhibits a reduction at α = 0.122 in the first block (AO labelled as S), which has the smallest contribution to the block (14.22%), but causes a 65.47% loss in normalization. When considering the Join-block, the contribution decreases to 6.02%, while the corresponding normalization loss is reduced to 29.06%. Initially, the block consists of 4 primitives forming the constructive part $\phi_+(r)$. After reduction, the block consists of 3 constructive components and this reduction is provided by default in the internal system library (A2).

Carbon. For the A1-type basis set normalization, carbon exhibits a reduction at α = 0.5215 and α = 0.1596 in the first block (AO labelled as S), which does not have the smallest contribution to the block (0.087% and 0.008%, respectively), and causes a 1.194% and −0.12% loss in normalization. When considering the Join-block, the contributions change to 0.058% and 0.005%, while the corresponding normalizations loss changes to 0.547% and −0.115%. Negative normalization loss indicates that the removed component was destructively interfering with the overall AO function, and its elimination leads to an increase in the total norm. Initially, the block consists of 8 primitives forming the constructive part $\phi_+(r)$, and 1 forming the destructive part $\phi_-(r)$. After reduction, the block consists of 7 constructive components only. In the internal system library (A2), all 8 components are present, with the destructive component reduced.

The next AO-labelled S block for carbon, although having the same α values, exhibits different reductions in the A1-type basis set normalization due to differing contraction coefficients. Carbon exhibits a reduction at α = 1000, α = 228 and α = 0.1596 in the block, whose contributions to the block are 6.324%, 10.352% and 4.517%, respectively, and causes a 0.007%, 0.079% and 75.216% loss in normalization. When considering the Join-block, the contributions change to 1.274%, 2.086% and 0.91%, and the corresponding normalization loss changes to −0.001%, −0.016% and 19.677%. Initially, the block consists of 2 primitives forming the constructive part $\phi_+(r)$, and 7 forming the destructive part $\phi_-(r)$. After reduction, the block consists of 3 constructive components and 4 destructive components. In the internal system library (A2), all 8 components are present, with 1 constructive component reduced (Table 1).

In the case of larger basis sets, greater and less intuitive reductions can be expected. For example, the carbon cc-pVTZ[5,6] case also shows a significant imbalance between constructive and destructive components, as presented in the ESI.†

Phosphorus. For the A1-type basis set normalization, phosphorus exhibits reductions at α = 1.818, α = 0.3372 and α = 0.1232 in the first block (AO labelled as S), which has contributions to the block of 0.009%, %0.008 and >0.001%, respectively, and causes a −0.1362%, 0.0122% and −0.0026% loss in normalization. When considering the Join-block, the contributions change to 0.005%, >0.001% and >0.001%, while the corresponding normalizations loss change to −0.058%, 0.024% and −0.01%. The components with α = 0.1818 and α = 0.1232 are the only ones with negative Gaussian contraction coefficient contributions, and were subsequently eliminated. Initially, the block consists of 10 primitives forming the constructive part $\phi_+(r)$, and 2 forming the destructive part $\phi_-(r)$. After reduction, the block consists of 9 constructive components without destructive components. In the internal system library (A2), all 11 components are present, with 1 destructive component reduced.

The second AO-labelled S block for phosphorus should have the same α values as for the first S block, but exhibits different reductions in the A1-type basis set normalization due to differing contraction coefficients. Phosphorus exhibits a reduction at α = 94 840, α = 14 220, α = 0.3372 and α = 0.1232 in the block, which results in contributions to the block of 2.181%, 4.037%, 0.095% and 0.012%, respectively, and causes a 3.135%, 5.86%,

Table 1 Norm loss and amplitude contribution per primitive Gaussian function for cc-pVDZ of H, C and P atoms

			δ_{loss}, %		$\delta_{contribution}$, %	
A	$\phi^{(l)}$	α	Block	Join-block	Block	Join-block
H	S	13.01	0.9082	0.3129	18.5385	7.8348
		1.962	15.6778	6.1664	31.4458	13.2897
		0.4446	68.0162	29.8528	35.7908	15.1260
		0.122	65.4686	29.0632	14.2248	6.0117
	S	0.122	—	51.5294	—	11.9937
	P	0.727	—	50.7382	—	45.7441
C	S	6665	0.0053	0.0002	4.7585	3.1704
		1000	0.1478	0.0057	8.8341	5.8857
		228	1.7935	0.0730	14.8105	9.8675
		64.71	11.7803	0.5400	21.6343	14.4138
		21.06	41.2350	2.4047	25.1787	16.7753
		7.495	67.2472	6.0494	18.9417	12.6199
		2.797	39.7860	6.0679	5.7477	3.8294
		0.5215	1.1944	0.5472	0.0870	0.0579
		0.1596	−0.1204	−0.1151	0.0075	0.0050
	S	6665	0.0002	−0.0000	3.3191	0.6689
		1000	0.0068	−0.0013	6.3244	1.2746
		228	0.0790	−0.0161	10.3523	2.0863
		64.71	0.5217	−0.1346	16.3915	3.3034
		21.06	1.3848	−0.6407	19.3767	3.9050
		7.495	−0.9100	−2.3578	20.9376	4.2196
		2.797	−7.2674	−2.9047	8.4826	1.7095
		0.5215	63.2844	18.5204	10.2985	2.0755
		0.1596	75.2160	19.6771	4.5174	0.9104
	S	0.1596	—	32.3308	—	1.5683
	P	9.439	2.4915	0.5202	20.6336	1.2746
		2.002	25.0107	5.1258	35.4482	2.1897
		0.5456	69.0712	17.2413	32.4600	2.0052
		0.1517	57.4163	15.9485	11.4583	0.7078
	P	0.1517	—	32.0338	—	1.5097
	D	0.55	—	32.0229	—	3.9667
P	S	94 840	0.0011	0.0000	3.1353	1.8169
		14 220	0.0330	0.0009	5.8598	3.3958
		3236	0.4426	0.0127	10.0105	5.8011
		917.1	3.5326	0.1063	15.6963	9.0962
		299.5	17.2745	0.5714	21.5746	12.5026
		108.1	47.9026	1.9171	23.4950	13.6156
		42.18	63.5880	3.5418	15.8078	9.1607
		17.28	31.6595	2.6245	4.2889	2.4855
		4.858	1.5508	0.2862	0.1219	0.0706
		1.818	−0.1362	−0.0578	0.0090	0.0052
		0.3372	0.0122	0.0239	0.0008	0.0004
		0.1232	−0.0026	−0.0102	0.0002	0.0001
	S	94 840	3.1353	−0.0000	2.1813	0.4956
		14 220	5.8598	−0.0003	4.0366	0.9171
		3236	10.0105	−0.0036	7.0493	1.6016
		917.1	15.6963	−0.0310	11.0007	2.4994
		299.5	21.5746	−0.1898	16.3825	3.7222
		108.1	23.4950	−0.7379	19.3444	4.3951
		42.18	15.8078	−2.0254	18.9770	4.3116
		17.28	4.2889	−1.4660	5.6376	1.2809
		4.858	0.1219	8.2875	9.8274	2.2328
		1.818	76.9352	12.6235	5.4570	1.2398
		0.3372	3.8829	1.1728	0.0945	0.0215
		0.1232	−0.5893	−0.2986	0.0117	0.0027
	S	94 840	0.0000	0.0000	1.8084	0.1360
		14 220	0.0002	0.0001	3.3552	0.2523
		3236	0.0025	0.0010	5.8412	0.4392
		917.1	0.0190	0.0084	9.1741	0.6897
		299.5	0.0886	0.0507	13.6330	1.0250
		108.1	0.1576	0.1969	16.4258	1.2349
		42.18	−0.3314	0.5350	16.3365	1.2282
		17.28	−0.7092	0.4414	5.3130	0.3994
		4.858	1.3662	−3.4933	11.0748	0.8326
		1.818	−19.393	−8.8649	10.1957	0.7665
		0.3372	60.5582	18.7893	4.8343	0.3635
		0.1232	70.7104	16.0662	2.0079	0.1510
	S	0.1232	—	27.8086	—	0.2736
	P	370.5	0.1269	0.0168	5.3800	0.4389
		87.33	2.2678	0.2291	13.9373	1.1370
		27.59	15.5405	1.3645	25.1540	2.0521
		10	47.1860	4.4096	29.7118	2.4239
		3.825	64.8942	7.9124	20.1593	1.6446
		1.494	33.4986	5.8694	5.5160	0.4500
		0.3921	1.4516	0.5302	0.1349	0.0110
		0.1186	−0.0870	−0.0632	0.0068	0.0006
	P	370.5	0.0060	−0.0041	4.2919	0.1067
		87.33	0.0929	−0.0547	10.7575	0.2673
		27.59	0.4846	−0.3601	20.8513	0.5182
		10	0.1021	−1.1660	23.6949	0.5888
		3.825	−5.1057	−2.5715	19.5532	0.4859
		1.494	−0.7868	−0.2182	0.6515	0.0162
		0.3921	66.5573	16.0722	14.1101	0.3506
		0.1186	75.0254	16.4273	6.0896	0.1513
	P	0.1186	—	27.6062	—	0.2659
	D	0.3730	—	28.7026	—	0.6280

3.883% and −0.589% loss in normalization. When considering the Join-block, the contributions change to 0.496%, 0.917%, 0.022% and 0.003%, and the corresponding normalizations loss change to $>-0.001\%$, $>-0.001\%$, 1.173% and −0.299%. Initially, the block consists of 4 primitives forming the constructive part $\phi_+(r)$, and 8 forming the destructive part $\phi_-(r)$. After reduction, the block consists of 2 constructive components and 6 destructive components and this number is smaller by 1 α value compared with the first AO-labelled S block. In the internal system library (A2), all 11 components are present, with 1 destructive component reduced.

The third AO-labelled S block for phosphorus should also have the same α values as for the first S block, but exhibits different reductions in the A1-type basis set normalization due to differing contraction coefficients also. Phosphorus exhibits a reduction at α = 94 840, α = 14 220, α = 299.5 and α = 0.1232 in the block, with contributions to the block of 2.808%, 3.355%, 13.633% and 2.008%, respectively, and causes a $>0.001\%$, $>0.001\%$, 0.089% and 70.71% loss in normalization. When considering the Join-block, the contributions change to 0.136%, 0.252%, 1.025% and 0.151%, and the corresponding normalizations loss changes to $>0.001\%$, $>0.001\%$, 0.051% and 16.067%. Initially, the block consists of 10 primitives forming the constructive part $\phi_+(r)$, and 2 forming the destructive part $\phi_-(r)$. After reduction, the block consists of 5 constructive components and 3 destructive components. In the internal system library (A2), all 11 components are present, with 1 constructive component reduced.

The first AO-labelled P block for phosphorus exhibits a reduction at α = 0.3921 and α = 0.1186, in the block, with contributions to the block of 0.135% and 0.007%, respectively, and causes a 1.452% and −0.087% loss in normalization. When considering the Join-block, the contributions change to 0.011% and 0.006%, and the corresponding normalizations loss changes to 0.53% and −0.063%. Initially, the block consists

of 7 primitives forming the constructive part $\phi_+(r)$, and 1 forming the destructive part $\phi_-(r)$. After reduction, the block consists of 6 constructive components without destructive components. In the internal system library (A2), all 7 components are present, with 1 destructive component reduced.

The second AO-labelled P block for phosphorus should have the same α values as for the first P block also, but exhibits different reductions in the A1-type basis set normalization due to differing contraction coefficients. Phosphorus exhibits a reduction at α = 370.5 and α = 0.1186 in the block, and its contributions to the block are 4.292% and 6.09%, respectively, and it causes a 0.006% and 75.025% loss in normalization. When considering the Join-block, the contributions change to 0.107% and 0.151%, and the corresponding normalizations loss changes to −0.004% and 16.427%. Initially, the block consists of 2 primitives forming the constructive part $\phi_+(r)$, and 6 forming the destructive part $\phi_-(r)$. After reduction, the block consists of 4 constructive components and 2 destructive components. In the internal system library (A2), all 7 components are present, with 1 constructive component reduced. This component results in a 75.025% loss in normalization, despite contributing only 6.09%. In contrast, destructive components with lower percentage contributions are not eliminated.

Using BasisSculpt, the actual norms of AO blocks used in the A1-type calculations were evaluated. Despite Gaussian applying internal normalization (A1), the resulting norms were not consistently equal to one. For example, the carbon atom P block reached 1.08, while phosphorus atom P blocks ranged from 1.01 to 1.13. These findings confirm that internal normalization in Gaussian software includes amplitude scaling, particularly for angular momentum components, which may affect sensitive properties.

Raman mode sensitivity to AO normalization for lycopene ν_1

CARs, such as lycopene (LYC), contain an extended polyene chain that supports delocalized π-conjugation, giving rise to strong Raman activity (Fig. 1). The vibrational modes are commonly labelled from ν_1 to ν_4 corresponding to characteristic C–C (carbon–carbon single bonds) and C=C (carbon–carbon double bonds) bond vibrations. LYC was chosen due to its relevance and recent theoretical and experimental characterization.[49–51,53]

Ground state, dipole moment, UV spectra, frequency and Raman activity calculations for LYC were performed using DFT (B3LYP/cc-pVDZ) with four different basis set normalization strategies: A1 (default Gaussian), A2 (system library), A3Exc (original cc-pVDZ from basis set exchange), and A4BS (BasisSculpt-renormalized). The LYC structures were optimized with the same DFT methodology as results analysed.

In all cases, the dipole moment (field-independent) remained constant at 0.5882 Debye. The total energy was identical for A1, A2, and A3Exc (−1557.93462692 Hartree), while for A4BS it differed slightly by −0.0001533472 eV, which is within the numerical noise range (0.0001 Hartree). Zero-point energy corrections were effectively the same, with A4BS differing only by 0.000001 Hartree per particle.

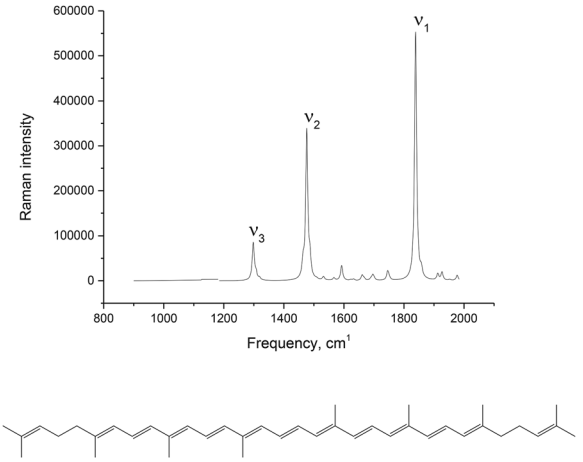

Fig. 1 Raman spectrum of lycopene showing three main peaks, with the chemical structure displayed below.

UV spectra were calculated using time-dependent density functional theory (TDDFT). In all cases, the lowest excited states were identical; for example, S_1 was calculated at 2.0866 eV, with an oscillator strength of 4.3861 and a major contribution (0.7104) from HOMO to LUMO.

Taking A1 as the reference, the ν_1 frequency (1553.6621 cm^{-1}) decreased by 0.0001 cm^{-1} for A2, increased by 0.0001 cm^{-1} for A3Exc, and increased by 0.0017 cm^{-1} for A4BS. The corresponding Raman activity changes were −1.1379, −12.1227, and +5.088, respectively.

For ν_2 (1191.1613 cm^{-1}), the frequency decreased by 0.0002 cm^{-1} for A2, decreased by 0.0001 cm^{-1} for A3Exc, and increased by 0.0008 cm^{-1} for A4BS. The Raman activity differences were +1.5469, +6.9930, and +1.5918.

For ν_3 (1012.7001 cm^{-1}), all basis sets yielded the same frequency, with a minor decrease of 0.0001 cm^{-1} for A4BS. Raman activity shifts were +3.2633, +35.0093, and +51.2232.

These results show that even minor deviations in AO normalization – particularly when destructive components are either retained or removed – can lead to measurable differences in Raman intensities, despite the fact that all calculations involved additional renormalization and yielded virtually identical total energies, UV spectra and vibrational frequencies.

Basis set normalization effect on *J*-coupling of P–P

Bis(diphenylphosphino)methane (dppm) (see Fig. 2) provides access to through-space phosphorus–phosphorus couplings, which are important in the context of quantum computing.[54–58] While in conventional quantum chemistry applications a sensitivity of 3–4 Hz is typically sufficient, quantum computing implementations often operate within sub-Hz precision, in the range of 0.1 Hz. Therefore, even small changes in orbital amplitude and spatial shape can significantly impact computed coupling constants, especially for heavier elements such as phosphorus.

Ground-state properties, dipole moments, and *J*-coupling values for dppm were calculated using DFT (B3LYP/cc-pVDZ) under four different basis set normalization strategies: A1 (default Gaussian), A2 (system library), A3Exc (original cc-pVDZ

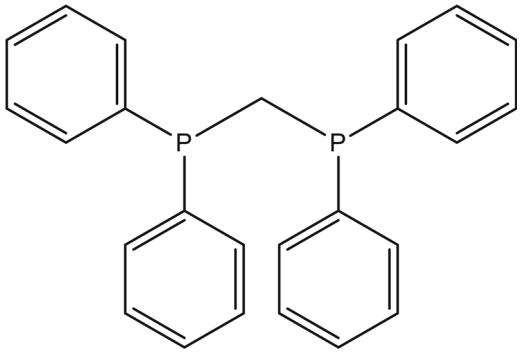

Fig. 2 Bis(diphenylphosphino)methane (dppm) chemical structure.

from basis set exchange), and A4BS (BasisSculpt-renormalized). Geometry optimization was performed with A1 to ensure consistent phosphorus–phosphorus distances across the first comparison group. To fully evaluate the effect of AO normalization on structure itself, an additional geometry optimization was performed using the A4BS basis set (labelled A4BSopt).

As expected, the field-independent dipole moment remained constant (1.6010 Debye) for A1, A2, A3Exc, and A4BS. However, in the A4BSopt case, the dipole moment increased to 1.6153 Debye. This change corresponds to a slight increase in the P–P distance by ∼0.01 Å (from 3.13586 Å to 3.14435 Å) indicating subtle structural rearrangements in the dppm geometry associated with renormalized AO amplitudes.

The total energies were identical (−1648.69310726 Hartree) for A2 and A3Exc, A1 differed marginally (−1648.69310645 Hartree), remaining within numerical noise. In contrast, A4BS and A4BSopt exhibited a decrease in total energy by 0.031 eV and 0.095 eV, respectively.

Total nuclear spin–spin coupling constants J(P–P) for A1, A2, A3Exc, and A4BS were found to be 100.89 Hz, 101.033 Hz, 101.034 Hz, and 101.247 Hz, respectively. This means that even at a fixed geometry (3.13586 Å), the J value varied by up to 0.4 Hz depending solely on the AO normalization strategy. In the A4BSopt case, where structural relaxation was allowed under renormalized AO functions, the J-coupling decreased more substantially to 95.322 Hz – highlighting a 6 Hz shift solely due to basis set normalization effects.

The results demonstrate that AO normalization is not merely a numerical refinement, but a physically impactful operation that directly influences computed spin–spin couplings. For systems involving heavy atoms such as phosphorus and properties requiring sub-Hz resolution, such as J(P–P), strict control over AO norms becomes essential. The observed variations confirm that even when total energies remain nearly identical, the shape and amplitude of AO functions – especially in normalized or destructively altered blocks – can significantly affect sensitive observables. Future work should explore scenarios in which package-level renormalization is fully disabled, as this may substantially alter the resulting physical predictions and reveal normalization-dependent effects more explicitly.

Computational methods

Basis set structure

The basis set database is presented in such a way that, for each atom, basis functions are grouped into several blocks corresponding to selected types of atomic orbitals (*e.g.*, S, P, D, *etc.*). This is described by the following equation:

$$\phi(\vec{r}) = \sum_k c_k \cdot N_k \cdot \mathrm{e}^{-\alpha_k r^2} \tag{13}$$

This is a contracted atomic orbital (AO), composed of primitive GTOs with primitive exponents α_k, normalization coefficients N_k, and contraction coefficients c_k, typically provided in the S and P (SP, D *etc.*) blocks of the basis set file. Each contracted block is expected to be normalized to unity.[2]

Implementation

The implementation (BasisSculpt) was written in Java and is available under a BSD license. It allows reading and analysing Gaussian-type basis sets, computing the norm of contracted atomic orbitals, and applying multiple normalization schemes. Projection-based normalization is included, along with a robust numerical fallback using a golden-section search for stability. The code supports BigDecimal arithmetic for high precision and is accessible *via* command-line or as a library module. BasisSculpt implementation retains both constructive and destructive contributions to the atomic orbital. When the discriminant in the analytical normalization equation is negative, the algorithm automatically resorts to numerical optimization.

DFT calculations

For computational analyses, the cc-pVDZ basis set[5,47] from the Gaussian 16 database[48] was used, as it allows automatic basis set reduction to be computed and analysed. The default approach (A1) has primitive eliminations while the non-eliminating approach (A2) has internal renormalization only. The unmodified reference (A3Exc) basis was also taken from the basis set exchange.[60] The renormalized basis set (A4BS) was generated using the BasisSculpt implementation with 64-digit mathematical precision. The normalization threshold was set to 1×10^{-10}, ensuring that each AO function was normalized to within ten decimal digits—matching the internal precision used by the Gaussian software and exposed to the user. It should be noted that in all cases, renormalization was performed prior to the computations, as it cannot be suppressed.[48]

For the chosen basis set sensitivity was calculated with energies, Raman spectra, and UV spectra of lycopene. The J-coupling was calculated for bis(diphenylphosphino)methane (dppm) as it has P–P interactions. All structures were optimised with the B3LYP[61] functional. All computations were performed by using Gaussian 16 Rev C.01.[48]

Conclusions

This study demonstrates that atomic orbital (AO) normalization – often treated as a technical detail – can have a physically

significant impact on computed molecular properties, particularly in cases involving heavy atoms and precision-sensitive observables. Through a comparison of four normalization strategies (A1, A2, A3Exc, and A4BS), it is shown that AO components, when removed or retained without phase-aware normalization, can measurably influence Raman intensities and spin–spin coupling constants, even when total energies remain numerically indistinguishable.

Projection-based normalization, incorporating both constructive and destructive contributions, was shown to be essential for preserving the physical form of AO blocks. The results reveal that default package-level normalization – such as in Gaussian – can lead to amplitude scaling, with AO norms varying up to ±13% across S and P blocks.

The vibrational frequency shifts remain negligible under different normalization schemes, but Raman intensities and spin–spin couplings (*e.g.*, *J*(P–P)) exhibit differences of up to 6 Hz. The AO normalization directly affects second- and fourth-order properties, which are critical for spectroscopic interpretation and quantum technology applications.

While basis set reduction does not significantly affect total energies or UV-vis spectra for larger molecules (*e.g.*, >20 atoms), the results of this study suggest otherwise for Raman intensities and spin–spin coupling constants. AO normalization influences the radial amplitude and curvature of contracted atomic orbitals, particularly near the nucleus. When constructive or destructive interference patterns are altered through primitive elimination or renormalization, the local electron density at the nucleus can change – even if the total molecular energy remains stable. These localized changes directly impact properties such as Fermi contact terms in NMR and Raman activity, which depend sensitively on electronic response near nuclei. This suggests that higher-order response properties, such as hyperpolarizabilities, may be even more susceptible to AO norm deviations and should be treated with particular care when using reduced or automatically normalized basis sets.

On the other hand, the use of larger basis sets – especially in contexts requiring high precision – is expected to increase. However, predefined basis set reduction may unintentionally degrade accuracy in such cases. For example, hydrogen bond interaction analysis presented in ref. 62 demonstrated accuracy limitations when reduction affects delicate intermolecular features.

Future work should focus on enabling control over, or fully disabling, internal normalization mechanisms in electronic structure packages to ensure full transparency and reproducibility in basis set behaviour. As the results indicate, it is sometimes insufficient to report only the DFT method and package version, as even different deployments of the same software version may apply distinct internal basis set reduction procedures. This highlights the need to explicitly report the applied basis set normalization strategy alongside computational results.

While the proposed framework in this study is based on contracted Gaussian primitives and is therefore formally compatible with ANO-type basis sets, its practical application requires further adjustments. ANO constructions often involve irregular contraction patterns, unbalanced block structures, and uncontracted diffuse functions optimized for correlated methods. Accordingly, block-wise normalization, primitive elimination, and contribution analysis must be adapted to handle flexible contraction schemes and extended numerical integration domains. These adjustments are technical in nature and do not limit the conceptual generality of the approach.

The approach proposed in this study is not intended as an alternative to normalization, but rather a method to preserve the constructive and destructive character of the AO block components during renormalization. Whether these contributions are critical depends not only on atomic type (*e.g.*, heavy elements) or molecular polarity, but also on the specific structure of the basis set – particularly in cases where destructive components compensate for large positive amplitudes. In such cases, improper reduction or reshaping may distort the intended shape of the contracted orbital.

Finally, it is important to emphasize that nearly all major quantum chemistry packages—including TURBOMOLE,[63] NWChem,[64] ORCA,[65–67] Q-Chem,[68] Molpro,[69,70] Dalton[71] and GAMESS[72]—perform internal normalization of user-supplied basis functions. Moreover, most quantum chemistry software packages include predefined reductions in their internal basis set databases. This is not specific to Gaussian 16 Rev. C.01; similar reductions are also present in the internal basis set database of NWChem. While NWChem documentation states that the basis set content is the responsibility of the system administrator, in practice, this means that the basis set database may vary depending on the specific installation or user's environment. Consequently, different installations of the same software version may include different internal basis sets. A similar situation applies to Gaussian, where internal corrections – such as modifications to the internal basis set database by the system administrator (*e.g.*, based on the basis set exchange) – can also vary. This leads to ambiguity regarding the origin and extent of predefined basis set reductions. This behaviour, while intended to ensure stability and consistency, may obscure the origin of differences in computed properties and complicate reproducibility unless explicitly documented. Therefore, reporting the applied normalization strategy, or disabling internal renormalization where possible, should be considered standard practice in high-precision computations.

Author contributions

CRediT: Mindaugas Macernis: conceptualization, data curation, formal analysis, funding acquisition, investigation, methodology, project administration, resources, software, supervision, validation, visualization, writing – review & editing.

Conflicts of interest

There are no conflicts to declare.

Data availability

The data supporting this article have been included in the GitHub repository at **https://github.com/BasisSculpt/BasisSculpt**, which contains input files, normalized basis sets, result summaries, and the source code of the BasisSculpt tool.

Acknowledgements

Supported by the Research Council of Lithuania (Grant No. S-MIP-23-48). Computations were performed on resources at the supercomputer "VU HPC" Saulėtekis of Vilnius University in Faculty of Physics.

References

1 T. Helgaker and P. R. Taylor, *Modern Electronic Structure Theory*, World Scientific, River Edge, 1995.
2 D. Young, *Computational Chemistry: A Practical Guide for Applying Techniques to Real-World Problems*, Wiley, 2001, p. 408.
3 S. F. Boys and A. C. Egerton, *Proc. R. Soc. London, Ser. A*, 1950, **200**, 542–554, DOI: **10.1098/rspa.1950.0036**.
4 E. R. Davidson and D. Feller, *Chem. Rev.*, 1986, **86**, 681–696, DOI: **10.1021/cr00074a002**.
5 T. H. Dunning, Jr., *J. Chem. Phys.*, 1989, **90**, 1007–1023, DOI: **10.1063/1.456153**.
6 R. A. Kendall, T. H. Dunning, Jr. and R. J. Harrison, *J. Chem. Phys.*, 1992, **96**, 6796–6806, DOI: **10.1063/1.462569**.
7 D. E. Woon and T. H. Dunning, Jr., *J. Chem. Phys.*, 1993, **98**, 1358–1371, DOI: **10.1063/1.464303**.
8 K. A. Peterson, R. A. Kendall and T. H. Dunning, Jr., *J. Chem. Phys.*, 1993, **99**, 9790–9805, DOI: **10.1063/1.465461**.
9 D. E. Woon and T. H. Dunning, Jr., *J. Chem. Phys.*, 1994, **100**, 2975–2988, DOI: **10.1063/1.466439**.
10 K. A. Peterson, D. E. Woon and T. H. Dunning, Jr., *J. Chem. Phys.*, 1994, **100**, 7410–7415, DOI: **10.1063/1.466884**.
11 D. E. Woon and T. H. Dunning, Jr., *J. Chem. Phys.*, 1995, **103**, 4572–4585, DOI: **10.1063/1.470645**.
12 A. K. Wilson, T. van Mourik and T. H. Dunning, *THEOCHEM*, 1996, **388**, 339–349, DOI: **10.1016/S0166-1280(96)80048-0**.
13 J. Almlöf and P. R. Taylor, *J. Chem. Phys.*, 1987, **86**, 4070–4077, DOI: **10.1063/1.451917**.
14 S. Huzinaga, *J. Chem. Phys.*, 1965, **42**, 1293–1302, DOI: **10.1063/1.1696113**.
15 R. F. Stewart, *J. Chem. Phys.*, 1969, **50**, 2485–2495, DOI: **10.1063/1.1671406**.
16 W. J. Hehre, R. F. Stewart and J. A. Pople, *J. Chem. Phys.*, 1969, **51**, 2657–2664, DOI: **10.1063/1.1672392**.
17 W. J. Hehre, R. Ditchfield, R. F. Stewart and J. A. Pople, *J. Chem. Phys.*, 1970, **52**, 2769–2773, DOI: **10.1063/1.1673374**.
18 F. Jensen, *Wiley Interdiscip. Rev.: Comput. Mol. Sci.*, 2013, **3**, 273–295, DOI: **10.1002/wcms.1123**.
19 P. O. Widmark, P. Å. Malmqvist and B. O. Roos, *Theor. Chim. Acta*, 1990, **77**, 291–306, DOI: **10.1007/BF01120130**.
20 C. W. Bauschlicher and P. R. Taylor, *Theor. Chim. Acta*, 1993, **86**, 13–24, DOI: **10.1007/Bf01113513**.
21 S. Saebø and P. Pulay, *Annu. Rev. Phys. Chem.*, 1993, **44**, 213–236, DOI: **10.1146/annurev.pc.44.100193.001241**.
22 R. Pouamerigo, M. Merchan, I. Nebotgil, P. O. Widmark and B. O. Roos, *Theor. Chim. Acta*, 1995, **92**, 149–181, DOI: **10.1007/Bf01114922**.
23 M. Filatov and D. Cremer, *J. Chem. Phys.*, 2005, **122**, 064104, DOI: **10.1063/1.1844298**.
24 A. G. Taube and R. J. Bartlett, *Collect. Czech. Chem. Commun.*, 2005, **70**, 837–850, DOI: **10.1135/cccc20050837**.
25 T. A. Barnes, J. D. Goodpaster, F. R. Manby and T. F. Miller, *J. Chem. Phys.*, 2013, **139**, 024103, DOI: **10.1063/1.4811112**.
26 C. Riplinger, B. Sandhoefer, A. Hansen and F. Neese, *J. Chem. Phys.*, 2013, **139**, 134101, DOI: **10.1063/1.4821834**.
27 R. Sure and S. Grimme, *J. Comput. Chem.*, 2013, **34**, 1672–1685, DOI: **10.1002/jcc.23317**.
28 D. I. Lyakh, *Int. J. Quantum Chem.*, 2014, **114**, 1607–1618, DOI: **10.1002/qua.24732**.
29 S. Grimme, J. G. Brandenburg, C. Bannwarth and A. Hansen, *J. Chem. Phys.*, 2015, **143**, 054107, DOI: **10.1063/1.4927476**.
30 R. Sure, J. G. Brandenburg and S. Grimme, *ChemOpen*, 2016, **5**, 94–109, DOI: **10.1002/open.201500192**.
31 M. Welborn, F. R. Manby and T. F. Miller, *J. Chem. Phys.*, 2018, **149**, 144101, DOI: **10.1063/1.5050533**.
32 M. Bensberg and J. Neugebauer, *J. Chem. Phys.*, 2019, **150**, 184104, DOI: **10.1063/1.5084550**.
33 P. F. Loos, B. Pradines, A. Scemama, J. Toulouse and E. Giner, *J. Phys. Chem. Lett.*, 2019, **10**, 2931–2937, DOI: **10.1021/acs.jpclett.9b01176**.
34 V. K. Prasad, A. Otero-de-la-Roza and G. A. DiLabio, *J. Chem. Theory Comput.*, 2022, **18**, 2913–2930, DOI: **10.1021/acs.jctc.2c00036**.
35 S. F. Boys and F. Bernardi, *Mol. Phys.*, 1970, **19**, 553–566, DOI: **10.1080/00268977000101561**.
36 A. Ichihara and R. Itoh, *Bull. Chem. Soc. Jpn.*, 1990, **63**, 958–960, DOI: **10.1246/bcsj.63.958**.
37 F. B. van Duijneveldt, J. G. C. M. van Duijneveldt-van de Rijdt and J. H. van Lenthe, *Chem. Rev.*, 1994, **94**, 1873–1885, DOI: **10.1021/cr00031a007**.
38 H. Kruse, L. Goerigk and S. Grimme, *J. Org. Chem.*, 2012, **77**, 10824–10834, DOI: **10.1021/jo302156p**.
39 F. R. Manby, M. Stella, J. D. Goodpaster and T. F. Miller, *J. Chem. Theory Comput.*, 2012, **8**, 2564–2568, DOI: **10.1021/ct300544e**.
40 R. M. Richard, K. U. Lao and J. M. Herbert, *J. Chem. Phys.*, 2013, **139**, 224102, DOI: **10.1063/1.4836637**.
41 C. Riplinger and F. Neese, *J. Chem. Phys.*, 2013, **138**, 034106, DOI: **10.1063/1.4773581**.
42 M. A. Collins and R. P. A. Bettens, *Chem. Rev.*, 2015, **115**, 5607–5642, DOI: **10.1021/cr500455b**.
43 J. Witte, J. B. Neaton and M. Head-Gordon, *J. Chem. Phys.*, 2017, **146**, 234105, DOI: **10.1063/1.4986962**.
44 B. Hégely, P. R. Nagy and M. Kállay, *J. Chem. Theory Comput.*, 2018, **14**, 4600–4615, DOI: **10.1021/acs.jctc.8b00350**.

45 M. Sharma and M. Sierka, *J. Chem. Theory Comput.*, 2022, **18**(11), 6892–6904, DOI: **10.1021/acs.jctc.2c00380**.
46 F. Jensen, *J. Chem. Theory Comput.*, 2024, **20**, 767–774, DOI: **10.1021/acs.jctc.3c01156**.
47 D. E. Woon and T. H. Dunning, *J. Chem. Phys.*, 1993, **98**, 1358–1371, DOI: **10.1063/1.464303**.
48 G. W. T. M. J. Frisch, H. B. Schlegel, *et al.*, *Gaussian 16, Revision C.01*, Gaussian, Inc., Wallingford CT, 2019.
49 L. Diska, A. Bockuviene, R. Gruskiene, T. Kavleiskaja, J. Sereikaite, G. Bankovskaite and M. Macernis, *Phys. Chem. Chem. Phys.*, 2025, **27**, 7874–7881, DOI: **10.1039/d5cp00034c**.
50 M. Macernis, S. Streckaite, R. Litvin, A. A. Pascal, M. J. Llansola-Portoles, B. Robert and L. Valkunas, *J. Phys. Chem. A*, 2022, **126**, 813–824, DOI: **10.1021/acs.jpca.1c09393**.
51 S. Streckaite, M. Macernis, F. Li, E. K. Trsková, R. Litvin, C. H. Yang, A. A. Pascal, L. Valkunas, B. Robert and M. J. Llansola-Portoles, *J. Phys. Chem. A*, 2020, **124**, 2792–2801, DOI: **10.1021/acs.jpca.9b11536**.
52 M. J. Llansola-Portoles, A. A. Pascal and B. Robert, *Carotenoids*, 2022, **674**, 113–135, DOI: **10.1016/bs.mie.2022.03.068**.
53 D. Gill, R. G. Kilponen and L. Rimai, *Nature*, 1970, **227**, 743–744, DOI: **10.1038/227743a0**.
54 P. O. Boykin, T. Mor, V. Roychowdhury, F. Vatan and R. Vrijen, *Proc. Natl. Acad. Sci. U. S. A.*, 2002, **99**, 3388–3393, DOI: **10.1073/pnas.241641898**.
55 N. A. Gershenfeld and I. L. Chuang, *Science*, 1997, **275**, 350–356, DOI: **10.1126/science.275.5298.350**.
56 D. G. Cory, A. F. Fahmy and T. F. Havel, *Proc. Natl. Acad. Sci. U. S. A.*, 1997, **94**, 1634–1639, DOI: **10.1073/pnas.94.5.1634**.
57 P. Pyykkö, *Theor. Chem. Acc.*, 2000, **103**, 214–216, DOI: **10.1007/s002149900011**.
58 J.-C. Hierso, D. Evrard, D. Lucas, P. Richard, H. Cattey, B. Hanquet and P. Meunier, *J. Organomet. Chem.*, 2008, **693**, 574–578, DOI: **10.1016/j.jorganchem.2007.11.035**.
59 F. B. Mallory, C. W. Mallory, K. E. Butler, M. B. Lewis, A. Q. Xia, E. D. Luzik, L. E. Fredenburgh, M. M. Ramanjulu, Q. N. Van, M. M. Francl, D. A. Freed, C. C. Wray, C. Hann, M. Nerz-Stormes, P. J. Carroll and L. E. Chirlian, *J. Am. Chem. Soc.*, 2000, **122**, 4108–4116, DOI: **10.1021/ja993032z**.
60 B. P. Pritchard, D. Altarawy, B. Didier, T. D. Gibson and T. L. Windus, *J. Chem. Inf. Model.*, 2019, **59**, 4814–4820, DOI: **10.1021/acs.jcim.9b00725**.
61 A. D. Becke, *J. Chem. Phys.*, 1993, **98**, 5648–5652, DOI: **10.1063/1.464913**.
62 M. Macernis, B. P. Kietis, J. Sulskus, S. H. Lin, M. Hayashi and L. Valkunas, *Chem. Phys. Lett.*, 2008, **466**, 223–226, DOI: **10.1016/j.cplett.2008.10.069**.
63 Y. J. Franzke, C. Holzer, J. H. Andersen, T. Begušić, F. Bruder, S. Coriani, F. Della Sala, E. Fabiano, D. A. Fedotov, S. Fürst, S. Gillhuber, R. Grotjahn, M. Kaupp, M. Kehry, M. Krstić, F. Mack, S. Majumdar, B. D. Nguyen, S. M. Parker, F. Pauly, A. Pausch, E. Perlt, G. S. Phun, A. Rajabi, D. Rappoport, B. Samal, T. Schrader, M. Sharma, E. Tapavicza, R. S. Treß, V. Voora, A. Wodyński, J. M. Yu, B. Zerulla, F. Furche, C. Hättig, M. Sierka, D. P. Tew and F. Weigend, *J. Chem. Theory Comput.*, 2023, **19**, 6859–6890, DOI: **10.1021/acs.jctc.3c00347**.
64 E. Aprà, E. J. Bylaska, W. A. de Jong, N. Govind, K. Kowalski, T. P. Straatsma, M. Valiev, H. J. J. van Dam, Y. Alexeev, J. Anchell, V. Anisimov, F. W. Aquino, R. Atta-Fynn, J. Autschbach, N. P. Bauman, J. C. Becca, D. E. Bernholdt, K. Bhaskaran-Nair, S. Bogatko, P. Borowski, J. Boschen, J. Brabec, A. Bruner, E. Cauët, Y. Chen, G. N. Chuev, C. J. Cramer, J. Daily, M. J. O. Deegan, T. H. Dunning Jr, M. Dupuis, K. G. Dyall, G. I. Fann, S. A. Fischer, A. Fonari, H. Früchtl, L. Gagliardi, J. Garza, N. Gawande, S. Ghosh, K. Glaesemann, A. W. Götz, J. Hammond, V. Helms, E. D. Hermes, K. Hirao, S. Hirata, M. Jacquelin, L. Jensen, B. G. Johnson, H. Jónsson, R. A. Kendall, M. Klemm, R. Kobayashi, V. Konkov, S. Krishnamoorthy, M. Krishnan, Z. Lin, R. D. Lins, R. J. Littlefield, A. J. Logsdail, K. Lopata, W. Ma, A. V. Marenich, J. Martin del Campo, D. Mejia-Rodriguez, J. E. Moore, J. M. Mullin, T. Nakajima, D. R. Nascimento, J. A. Nichols, P. J. Nichols, J. Nieplocha, A. Otero-de-la-Roza, B. Palmer, A. Panyala, T. Pirojsirikul, B. Peng, R. Peverati, J. Pittner, L. Pollack, R. M. Richard, P. Sadayappan, G. C. Schatz, W. A. Shelton, D. W. Silverstein, D. M. A. Smith, T. A. Soares, D. Song, M. Swart, H. L. Taylor, G. S. Thomas, V. Tipparaju, D. G. Truhlar, K. Tsemekhman, T. Van Voorhis, Á. Vázquez-Mayagoitia, P. Verma, O. Villa, A. Vishnu, K. D. Vogiatzis, D. Wang, J. H. Weare, M. J. Williamson, T. L. Windus, K. Woliński, A. T. Wong, Q. Wu, C. Yang, Q. Yu, M. Zacharias, Z. Zhang, Y. Zhao and R. J. Harrison, *J. Chem. Phys.*, 2020, **152**, 184102, DOI: **10.1063/5.0004997**.
65 F. Neese, *Wiley Interdiscip. Rev.: Comput. Mol. Sci.*, 2012, **2**, 73–78, DOI: **10.1002/wcms.81**.
66 F. Neese, *Wiley Interdiscip. Rev.: Comput. Mol. Sci.*, 2018, **8**, e1327, DOI: **10.1002/wcms.1327**.
67 F. Neese, F. Wennmohs, U. Becker and C. Riplinger, *J. Chem. Phys.*, 2020, **152**, 224108, DOI: **10.1063/5.0004608**.
68 E. Epifanovsky, A. T. B. Gilbert, X. Feng, J. Lee, Y. Mao, N. Mardirossian, P. Pokhilko, A. F. White, M. P. Coons, A. L. Dempwolff, Z. Gan, D. Hait, P. R. Horn, L. D. Jacobson, I. Kaliman, J. Kussmann, A. W. Lange, K. U. Lao, D. S. Levine, J. Liu, S. C. McKenzie, A. F. Morrison, K. D. Nanda, F. Plasser, D. R. Rehn, M. L. Vidal, Z.-Q. You, Y. Zhu, B. Alam, B. J. Albrecht, A. Aldossary, E. Alguire, J. H. Andersen, V. Athavale, D. Barton, K. Begam, A. Behn, N. Bellonzi, Y. A. Bernard, E. J. Berquist, H. G. A. Burton, A. Carreras, K. Carter-Fenk, R. Chakraborty, A. D. Chien, K. D. Closser, V. Cofer-Shabica, S. Dasgupta, M. de Wergifosse, J. Deng, M. Diedenhofen, H. Do, S. Ehlert, P.-T. Fang, S. Fatehi, Q. Feng, T. Friedhoff, J. Gayvert, Q. Ge, G. Gidofalvi, M. Goldey, J. Gomes, C. E. González-Espinoza, S. Gulania, A. O. Gunina, M. W. D. Hanson-Heine, P. H. P. Harbach, A. Hauser, M. F. Herbst, M. Hernández Vera, M. Hodecker, Z. C. Holden, S. Houck, X. Huang, K. Hui, B. C. Huynh, M. Ivanov, Á. Jász, H. Ji, H. Jiang, B. Kaduk, S. Kähler, K. Khistyaev, J. Kim, G. Kis, P. Klunzinger, Z. Koczor-Benda, J. H. Koh, D. Kosenkov, L. Koulias, T. Kowalczyk, C. M. Krauter, K. Kue, A. Kunitsa, T. Kus, I. Ladjánszki, A. Landau, K. V. Lawler, D. Lefrancois, S. Lehtola, R. R. Li,

Y.-P. Li, J. Liang, M. Liebenthal, H.-H. Lin, Y.-S. Lin, F. Liu, K.-Y. Liu, M. Loipersberger, A. Luenser, A. Manjanath, P. Manohar, E. Mansoor, S. F. Manzer, S.-P. Mao, A. V. Marenich, T. Markovich, S. Mason, S. A. Maurer, P. F. McLaughlin, M. F. S. J. Menger, J.-M. Mewes, S. A. Mewes, P. Morgante, J. W. Mullinax, K. J. Oosterbaan, G. Paran, A. C. Paul, S. K. Paul, F. Pavošević, Z. Pei, S. Prager, E. I. Proynov, Á. Rák, E. Ramos-Cordoba, B. Rana, A. E. Rask, A. Rettig, R. M. Richard, F. Rob, E. Rossomme, T. Scheele, M. Scheurer, M. Schneider, N. Sergueev, S. M. Sharada, W. Skomorowski, D. W. Small, C. J. Stein, Y.-C. Su, E. J. Sundstrom, Z. Tao, J. Thirman, G. J. Tornai, T. Tsuchimochi, N. M. Tubman, S. P. Veccham, O. Vydrov, J. Wenzel, J. Witte, A. Yamada, K. Yao, S. Yeganeh, S. R. Yost, A. Zech, I. Y. Zhang, X. Zhang, Y. Zhang, D. Zuev, A. Aspuru-Guzik, A. T. Bell, N. A. Besley, K. B. Bravaya, B. R. Brooks, D. Casanova, J.-D. Chai, S. Coriani, C. J. Cramer, G. Cserey, A. E. DePrince, III, R. A. DiStasio, Jr., A. Dreuw, B. D. Dunietz, T. R. Furlani, W. A. Goddard, III, S. Hammes-Schiffer, T. Head-Gordon, W. J. Hehre, C.-P. Hsu, T.-C. Jagau, Y. Jung, A. Klamt, J. Kong, D. S. Lambrecht, W. Liang, N. J. Mayhall, C. W. McCurdy, J. B. Neaton, C. Ochsenfeld, J. A. Parkhill, R. Peverati, V. A. Rassolov, Y. Shao, L. V. Slipchenko, T. Stauch, R. P. Steele, J. E. Subotnik, A. J. W. Thom, A. Tkatchenko, D. G. Truhlar, T. Van Voorhis, T. A. Wesolowski, K. B. Whaley, H. L. Woodcock, III, P. M. Zimmerman, S. Faraji, P. M. W. Gill, M. Head-Gordon, J. M. Herbert and A. I. Krylov, *J. Chem. Phys.*, 2021, **155**, 084801, DOI: **10.1063/5.0055522**.

69 H.-J. Werner, P. J. Knowles, F. R. Manby, J. A. Black, K. Doll, A. Heßelmann, D. Kats, A. Köhn, T. Korona, D. A. Kreplin, Q. Ma, T. F. Miller, III, A. Mitrushchenkov, K. A. Peterson, I. Polyak, G. Rauhut and M. Sibaev, *J. Chem. Phys.*, 2020, **152**, 144107, DOI: **10.1063/5.0005081**.

70 H.-J. Werner, P. J. Knowles, G. Knizia, F. R. Manby and M. Schütz, *Wiley Interdiscip. Rev.: Comput. Mol. Sci.*, 2012, **2**, 242–253, DOI: **10.1002/wcms.82**.

71 K. Aidas, C. Angeli, K. L. Bak, V. Bakken, R. Bast, L. Boman, O. Christiansen, R. Cimiraglia, S. Coriani, P. Dahle, E. K. Dalskov, U. Ekström, T. Enevoldsen, J. J. Eriksen, P. Ettenhuber, B. Fernández, L. Ferrighi, H. Fliegl, L. Frediani, K. Hald, A. Halkier, C. Hättig, H. Heiberg, T. Helgaker, A. C. Hennum, H. Hettema, E. Hjertenæs, S. Høst, I.-M. Høyvik, M. F. Iozzi, B. Jansík, H. J. A. Jensen, D. Jonsson, P. Jørgensen, J. Kauczor, S. Kirpekar, T. Kjærgaard, W. Klopper, S. Knecht, R. Kobayashi, H. Koch, J. Kongsted, A. Krapp, K. Kristensen, A. Ligabue, O. B. Lutnæs, J. I. Melo, K. V. Mikkelsen, R. H. Myhre, C. Neiss, C. B. Nielsen, P. Norman, J. Olsen, J. M. H. Olsen, A. Osted, M. J. Packer, F. Pawlowski, T. B. Pedersen, P. F. Provasi, S. Reine, Z. Rinkevicius, T. A. Ruden, K. Ruud, V. V. Rybkin, P. Sałek, C. C. M. Samson, A. S. de Merás, T. Saue, S. P. A. Sauer, B. Schimmelpfennig, K. Sneskov, A. H. Steindal, K. O. Sylvester-Hvid, P. R. Taylor, A. M. Teale, E. I. Tellgren, D. P. Tew, A. J. Thorvaldsen, L. Thøgersen, O. Vahtras, M. A. Watson, D. J. D. Wilson, M. Ziolkowski and H. Ågren, *Wiley Interdiscip. Rev.: Comput. Mol. Sci.*, 2014, **4**, 269–284, DOI: **10.1002/wcms.1172**.

72 G. M. J. Barca, C. Bertoni, L. Carrington, D. Datta, N. De Silva, J. E. Deustua, D. G. Fedorov, J. R. Gour, A. O. Gunina, E. Guidez, T. Harville, S. Irle, J. Ivanic, K. Kowalski, S. S. Leang, H. Li, W. Li, J. J. Lutz, I. Magoulas, J. Mato, V. Mironov, H. Nakata, B. Q. Pham, P. Piecuch, D. Poole, S. R. Pruitt, A. P. Rendell, L. B. Roskop, K. Ruedenberg, T. Sattasathuchana, M. W. Schmidt, J. Shen, L. Slipchenko, M. Sosonkina, V. Sundriyal, A. Tiwari, J. L. Galvez Vallejo, B. Westheimer, M. Wloch, P. Xu, F. Zahariev and M. S. Gordon, *J. Chem. Phys.*, 2020, **152**, 154102, DOI: **10.1063/5.0005188**.

